Influence of γ-irradiation and ultrasound treatment on current mechanism in Au-SiO$_2$-Si structure

A.M. Gorb, O.A. Korotchenkov, O.Ya. Olikh*, A.O. Podolian, R.G. Chupryna

Faculty of Physics, Taras Shevchenko National University of Kyiv, Kyiv 01601, Ukraine

ARTICLE INFO

ABSTRACT

The effect of ^{60}Co γ-irradiation ($5 \cdot 10^7$ rad) and ultrasound treatment (4 MHz, 2 W/cm^2, up to 60 min) on current-voltage characteristics is experimentally investigated in an Au-SiO$_2$-Si structure. The change in the current mechanism is analysed in terms of a modifying defect system. The irradiation is shown to enhance the space charge limited current and trap-assisted tunneling current. Experimental observations of the acoustically induced low temperature annealing of the P_b and E' centers, which causes the partial recovery of irradiated silicon MOS structure characteristics, are highlighted.

1. Introduction

It is well known that defects are crucial for semiconductor devices performance. Thus, electrical characteristics of metal–oxide–semiconductor (MOS) structure are extremely sensitive to the interface state density. The formation of radiation defects (RDs) near the interface is therefore very harmful for device fabrications and frequently leads to a change in current mechanisms [1–6]. It is known that elastic acoustic vibrations can effectively interact with RDs and offer an interesting approach in trying to develop novel tools to controllably manipulate the defect properties. For example, RDs were annealed by acoustic wave treatments at a much lower temperature compared to that used for thermal annealing. Such phenomenon was observed in Si [7–9], Ge [10], semiconducting compounds [11,12], and alkali halides [13]. Usually, the suggested mechanism deals with a decay of radiation-formed complexes and acoustically induced (AI) diffusion of defects to a sink.

Moreover, the ultrasound treatment (UST) can recover defect-related electronic parameters of irradiated barrier structures. For example, the "active" ultrasound effects were observed in solar cells [14–17], light-emitting diodes (LEDs) [18,19], and Schottky diodes [20,21]. Furthermore, the AI modification of interface defects [22–24] and minority carrier lifetimes [25–27] were reported in industrially important Si-SiO$_2$ system.

Particular attention was paid to the UST of silicon MOS structures irradiated by ^{60}Co γ-rays [28,29]. Utilising capacitance-voltage measurements, the authors observed the post-UST decrease of the radiation-induced charge in dielectric layers of the structures. They also detected decreased carrier lifetimes in Si, whereas the growth of surface recombination rates considered insignificant [28,29].

The first aim of our work is to experimentally investigate the influence of UST on the charge transfer in irradiated Au-SiO$_2$-Si structures. In contrast to the cited study [28,29], our results are obtained i) for structures with a significantly higher RD concentration in the conductive layer (see Section 2); ii) for the diode operating in the current mode. It should be noted that some of our results have been reported earlier [27]. However, this paper is focused on evolving more detailed models that describe the modification of current mechanisms and the evolution of the defect structure, which are caused by irradiation and UST.

On the other hand, the efficiency of Si solar cell is restricted by the recombination of carriers [30]. The silicon surface is often highly recombination active due to the abundance of dangling bonds. The number of band-gap states can be reduced by introducing a dielectric coating. The anneal is one of the most effective methods of passivation of Si-SiO$_2$ interface [30–32]. This reaction was reported to release atomic hydrogen that is then free to diffuse across the oxide and passivate dangling bonds at the oxide-silicon interface [31–33]. The results presented in this work demonstrate the feasibility of the acoustically induced enhancement of hydrogen diffusion. Therefore, acousto-anneal can be used as an effective processing step in fabricating devices based on the MOS technology.

* Corresponding author.
  E-mail address: olikh@univ.kiev.ua (O.Y. Olikh).

2. Experimental and calculation details

Experiments were performed on n-type (111)-oriented crystalline float-zone Si with residual boron (B) impurity concentration of about 10^{12} cm^{-3} and doping phosphorus (P) impurity concentration of $2 \cdot 10^{12}$ cm^{-3}. The corresponding resistivity is 4000 $\Omega \cdot$cm. A bulk silicon material was divided into several rectangular-shaped samples of approximately $1 \times 5 \times 10$ mm^3. The MOS structures were formed by chemical etching of the upper Si surfaces using HF-HNO$_3$-CH$_3$COOH solutions (HF:HNO$_3$:CH$_3$COOH = 3: 5: 3), followed by the surface oxidation due to the exposure to ambient air for 24 h at room temperature and the Au vacuum evaporation. As a result, SiO$_2$ layer with a thickness of 10–15 Å [34–36] was formed. According Sze and Lee [37], the thickness of the depletion layer is about 10 μm. GaZn-eutectic Ohmic contacts were rubbed on the bottom surfaces of the samples.

The samples were γ-irradiated (^{60}Co source) at nominal room temperature to the dose of $5 \cdot 10^7$ rad. The measurement on the reference bulk sample shown that the conductivity has been reduced to about 0.5 of the initial value after irradiation. As mentioned above, the ultrasound influence on γ-irradiated Si-SiO$_2$ structure, created by thermal oxidation, has been previously investigated [28,29]. However, we used higher irradiation dozes, up to $5 \cdot 10^7$ rad, which were not more than 10^6 rad in Refs. [28,29]. Second, the sample resistivity was much greater in our case (4000 $\Omega \cdot$cm in contrast to 0.2–0.5 $\Omega \cdot$cm reported in Refs. [28,29]); therefore, the non-ionizing energy losses were larger as well. Third, it is known [38] that the density of γ-induced interface defects depends on substrate orientation, and an irradiation of (111)-oriented Si-SiO$_2$ structure (our case) leads to higher RD concentrations compared to that for the (100) substrate employed by Parchinskii et al. [28,29]. Therefore, much more heavy structure degradation is expected in our case.

UST was done by attaching the piezoelectric transducer to one side of the sample. An epoxy glue was used as the bonding medium, providing the rigid coupling of the transducer to the sample. The thickness resonance of the transducers was 4 MHz. A radio-frequency voltage supplied from a generator drives the transducer, resulting in vibrations of the coupled transducer-sample system. UST was carried out by a two consecutive loading-unloading cycles, 30 min each; so the total UST time t_{UST} was equal to either 30 min or 60 min. The acoustic energy flux density W_{US} in Si was about 2 W/cm^2. The sample temperature was measured with a copper-constantan thermocouple directly attached to the surface and did not exceed 350 K. The more details about the sample and UST setup are given elsewhere [27].

The initial Au-SiO$_2$-Si structure, γ-irradiated structure, and both irradiated and ultrasonically treated structure were investigated by using the current-voltage (I-V) technique. The forward and reverse bias characteristics were measured at 300 K in the current range from 10^{-9} to 10^{-3} A with a voltage step of 0.01 V. To identify the current mechanism in the irradiated structure, I-V characteristics were measured over a temperature range $\sim$300–340 K before UST.

The data non-linear fitting was done by using the method of modified artificial bee colony [39].

3. Results and discussion

Fig. 1 shows the I-V characteristics taken in the initial and irradiated Au-SiO$_2$-Si structures as well as after the sequent USTs. It is seen that the I-V curve for the non-irradiated sample is typical for the Schottky diode: The forward current is caused by a thermionic emission (TE) over the potential barrier, the reverse current value is determined by the barrier height lowering, which occurs due to the electric field ($\log I \sim V^{1/2}$) [40,41]. The forward branch was modeled by fitting the following equation to the experimental data plotted in Fig. 1 [40]

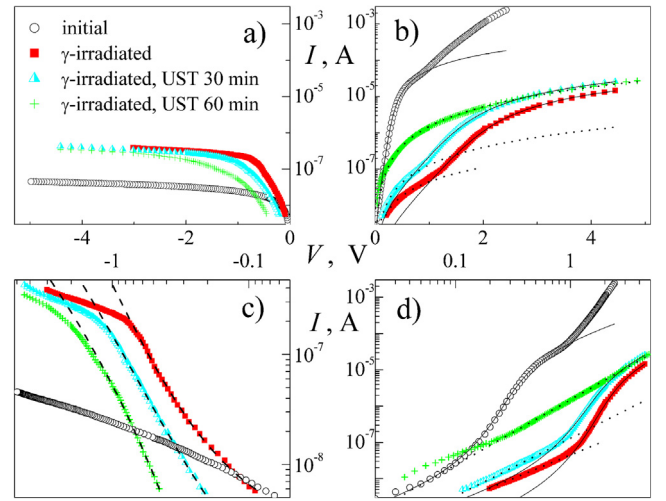$$I = I_s \left\{ \exp \left[\frac{q(V - IR_s)}{nkT} \right] - 1 \right\}, \tag{1}$$

Fig. 1. The logarithmical (a, b) and double-logarithmical (c, d) plots of the reverse (a, c) and forward (b, d) I-V characteristics for Au-SiO$_2$-Si structure before and after γ-irradiation and UST. T = 300 K. The marks are the experimental results, and the solid, dashed, and dotted lines are the TE, TAT, and SCLC fitted curves using Eqs. (1), (7), and (3), respectively.

Table 1
Extracted parameters for the Au-SiO$_2$-Si structure.

Structure status				
γ-irradiation	−	+	+	+
UST	−	−	+	+
t_{UST} (min)	0	0	30	60
Parameter				
I_s (10^{-9}A)	3.3 ± 0.3	1.1 ± 0.2	4.9 ± 0.5	−
R_s (10^4)	1.1 ± 0.2	13 ± 1	9 ± 1	−
n	1.7 ± 0.1	10.3 ± 0.2	9.9 ± 0.2	−
m_F	−	1.30 ± 0.05	1.6 ± 0.05	1.8 ± 0.05
I_0 (10^{-8} A)	−	5 ± 1	13 ± 2	150 ± 10
$I_{0,TAT}$ (a.u.)	−	1	0.14 ± 0.03	0.04 ± 0.01
U_d (V)	−	0.7 ± 0.1	0.44 ± 0.05	0.12 ± 0.05
R_{TAT} (a.u.)	−	1	0.54 ± 0.05	0.33 ± 0.04
$K_{RECT, 0.5V}$	800 ± 100	0.22 ± 0.03	1.3 ± 0.2	5.4 ± 0.8

where I_s is the saturation current, R_s is the series resistance, n is the ideality factor, the other symbols have their usual meanings. The fitting results are shown by solid lines in Fig. 1(b) and (d), the resulting parameter values are listed in Table 1. It should be noted that the presence of the oxide layer does not allow the barrier height to be determined only using the I_s value, since the carrier tunneling must also be taken into account [42,43].

The experimental forward current value obtained in the non-irradiated structure exceeds the one expected from Eq. (1) at high bias; see Fig. 1. The extra current is most likely to be due to the carrier tunneling through the SiO$_2$ layer. The tunneling current can be given by [40,44]:

$$\ln \left(\frac{I}{F_m^2} \right) \propto -\frac{4\sqrt{2m^*}(qE_{\text{eff}})^{3/2}}{3\hbar q F_m}, \tag{2}$$

where F_m is the electric field, E_{eff} is the effective tunneling energy. The linearity of the Fowler-Nordheim plot (Fig. 2) indicates of reasonable assumption for the excess current mechanism. It was taken into account when plotting that the electric field in a oxide layer is proportional to the applied voltage $F_m \propto V$.

As shown in Fig. 1, the γ-irradiation has a considerable effect on the I-V curve, which is obviously due to a modified current mechanism. Thus, the forward current decreases after irradiation and the I-V dependence, which is expected in the TE model, is observed only at
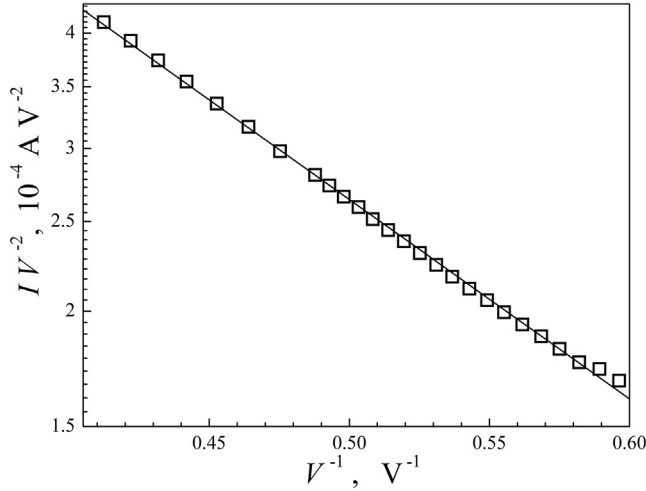
Fig. 2. The Fowler-Nordheim plot of the forward branch for the non-irradiated Au-SiO₂-Si structure at $V > 1, 6$ V. The line is the least-squares linear fitting result.

Fig. 3. Temperature dependence of SCLC-current for γ-irradiated Au-SiO₂-Si structure before UST at $V = 0, 4$ V. Inset: Temperature dependence of power-law parameter. Lines are the least-squares linear fits.

$V > 1$ V. It should be emphasised that the radiation-induced current reduction in MOS structure was previously reported [45].

The region $V > 1$ V fitted by Eq. (1) shows that the irradiation can significantly increase both the series resistance and ideality factor; see Table 1. In our opinion, increase in R_s can be explained by the γ-irradiation effects in bulk Si. Pintilie et al. [46] investigated the influence of γ-irradiation ($9 \cdot 10^7$ rad) on silicon (Fz-Si, 4 kΩ·cm), demonstrating that the known complexes VO$_i$, C$_i$ C$_s$, H-center (V₂O$_i$), Γ-center, and interstitial defect $I^{0/-}$ are the main radiation defects involved. $I^{0/-}$ is a secondary defect and its appearance leads to compensation (inversion) of electrical conductivity [46]. It may be suggested that this defect is responsible for varying series resistance R_s. In turn, the increase in R_s to about 13 times causes the reduction of the voltage drop in the dielectric layer. As a result, the electric field intensity was ceased to be sufficient for effective Fowler-Nordheim tunneling and such current component was not observed after irradiation. The increase in the ideality factor can also be explained by formation of RDs and results in observed decreasing of the TE current.

Fig. 1(d) shows that the forward I-V characteristic of irradiated structures at low biases ($V < 1$ V) is quite well described by a power law

$$I = I_0 V^{m_{\mathrm{F}}}, \tag{3}$$

where $m_{\mathrm{F}} = \frac{V}{I} \frac{\partial I}{\partial V}$ is the power-law parameter. The relation (3) is typical for the space charge limited current (SCLC) [47–49] with the value of m_{F} being the energy distribution of traps emitting carriers. For instance, the value $m_{\mathrm{F}} \approx 1.3$, which is observed in our structure after γ-irradiation and before UST corresponds to the exponentially distributed traps. It is known [47–49] that I_0 depends on the total trap concentration N_t as

$$I_0 \sim 1/N_t^{m_{\mathrm{F}}-1}, \tag{4}$$

and the temperature dependence of the power-law parameter is given by

$$m_{\mathrm{F}} = 1 + T_c/T, \tag{5}$$

where T_c is the trap energy distribution parameter. This can be related to the trap concentration per unit energy range located at an energy E above the valence band maximum as $P(E) = \frac{N_t}{kT_c} \exp(-\frac{E}{kT_c})$. The observed linearity of the temperature dependence of m_{F} (inset in Fig. 3) supports the above assumption that the SCLC would be taken into account to explain the experiments. It is also known [48] that the SCLC conduction should become important when the density of injected carriers is much larger than the density of thermally generated carriers. Therefore, SCLC appearance be expected in our structures fabricated on Si substrates with a high resistivity.
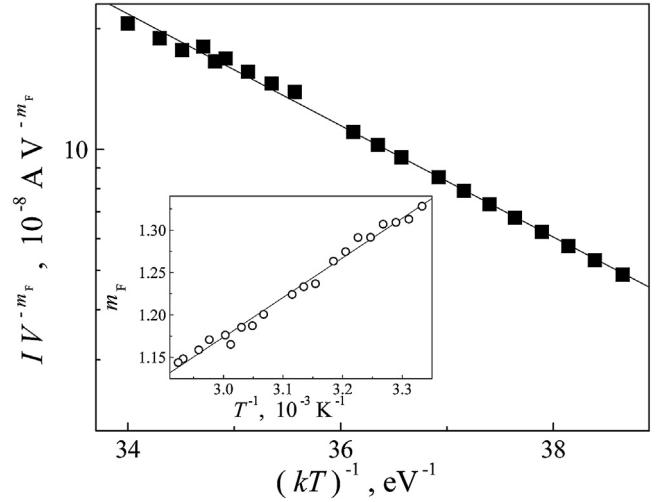
The SCLC current-voltage relation is often written as [48]

$$I(V, T) = C \exp\left(-\frac{E_x}{kT}\right) V^{m_{\mathrm{F}}(T)}, \tag{6}$$

where C is the constant and E_x is the activation energy linked to the trap level. Taking into account Eq. (5), one gets the temperature dependence of the forward current shown in Fig. 3. It is seen that the experimental data points in Fig. 3 can be fitted well by Eq. (6) (line in Fig. 3) with the fitting parameter $E_x = (0, 32 \pm 0, 01)$ eV.

Let's consider radiation defects, which can result in SCLC. Some notes are appropriate. Firstly, the low temperature and low partial oxygen pressure used here form thin SiO₂ layers. Meanwhile, same radiation defects are known [50] to be created in both thin and thick layers. Secondly, the hydrogen content is the key factor for generating electrically active RDs in Si—MOS structures [50]. Native SiO₂ layers are known to be enriched with atomic hydrogen [34,38].

The γ-irradiation of Si-SiO₂ structures is known [38] to lead to a stress relaxation, trap filling, and charged defect generation. It is believed [51,52] that the negative charge is trapped at the interface while the positive charge accumulates in the oxide bulk. In particular, the irradiation results in breaking of the $\equiv$Si $-$ H bonds at Si-SiO₂ interface [53–55]. The unsaturated bonds $\equiv$Si$-$ act as electronic traps. The configuration of these defects depends appreciably on the silicon substrate orientation. It is widely believed [56] that the P_b centers appear at the (111)-oriented substrate interface, whereas the P_{b1} and P_{b0} centers are typical for the (100)-oriented substrates. Both P_{b0} and P_{b1} are chemically identical to P_b, although the difference in their electrical activity has been observed [56]. The anneal temperature is about 150 °C [55] for P_b.

The γ-ray irradiation with doses above $5 \cdot 10^5$ rad leads to non-monotonic energy distribution of interface levels in n-Si—SiO₂ structure [38]. According to Parchinskii et al. [57], the highest density of surface states is observed at $E_c - (0, 32 \pm 0, 04)$ eV, coinciding with the value of E_x obtained from Fig. 3.

In our opinion, the P_b traps, being main electronic traps, are involved in SCLC process at low forward bias in irradiated structures. Besides, the negative charge accumulated at the interface results both in increasing the barrier height and decreasing the TE current.

Fig. 1(b) and (d) show that UST causes an increase in the space charge limited current. We used Eq. (3) to fit experimental I-V curves of ultrasonically treated structures. The resulting fitting parameters are summarized in Table 1. According to Eq. (4), the detected increase in the I_0 value is evidently due to AI decreased P_b concentration. It should

be pointed out that acousto-annealing takes place at rather low temperatures, which do not exceed ≈80 °C.

On the one hand, the acousto-defect interaction in Si has been reported [58–60,23,61,62] to cause atomic diffusion, transformation of native and impurity defects, modification of interior surface states, and appearance of new defects. On the other hand, the P_b center annealing is known [63,64] to deal with the passivation of dangling bonds at the oxide-silicon interface by hydrogen atoms. Therefore, the AI diffusion of hydrogen can be attempted to explain our results. It should be stressed that similar phenomenon has previously been reported [22,65,66].

Table 1 shows that UST leads to the increase of m_F. According to Eq. (5), the m_F increment deals with the increase in T_c value as well as narrowing of the distribution of trap levels. So, it is known [48] that $m_F = 2$ is observed in the case of single-energy traps. Therefore, the acousto-annealing selectivity is evidenced by the observed narrowing, so that atomic hydrogen can be captured only by certain dangling bonds during UST.

In our opinion, the key parameter for the AI bond passivation is an existence of mechanical stress, which is generally non-uniform at the interface. The impurity diffusivity in turn depends on the stress [67]. The varying mechanical stress at acoustic loading can displace the hydrogen atoms, and the efficiency of AI passivation is therefore determined by the strain field around the defect.

The acousto-annealing of the P_b centers decreases the negative interface charge and results both in partial recovery of the barrier height and increase in the TE current value; see Table 1. The AI decrease in R_s is therefore due to annealing of RDs ($I^{0/-}$ center) in the bulk of silicon.

The γ-released hydrogen atoms are potentially hazardous because of these mobile species are able [51,68,53,54] i) to interact with hydrogen bonded at the Si/SiO$_2$ interface and thus to give rise to additional P_b centers; ii) to move inside the semiconductor bulk and to produce generation-recombination sites and deactivate boron in the Si substrate; iii) to migrate within oxide thus creating the E' centers. It is believed [63,51] that the E' center is due to broken ≡Si − O bonds, resulting from the oxygen vacancy in SiO$_2$ and trapping positive charge. It has been concluded [55,51] that the E' centers dominate the hole trapping processes in oxide films grown on silicon. In 10^7 rad γ-irradiated silicon, the total concentration of E' is about 10^{18} cm^{-3}, but the centers are non-uniformly distributed over the oxide layer depth and largest concentrations are expected near the Si/SiO$_2$ interface [38]. The broken ≡Si − O bonds do not recover at room temperature and the temperature of E' annealing is equal to 200 °C [53,63,55].

The generation of E' centers is accompanied by a large (several orders of magnitude) increase in leakage currents [53,68,55]. The leakage currents are likely caused by inelastic tunneling of conduction band electrons to defect centers in the oxide near the Si/SiO$_2$ boundary [55,54,68]. In our opinion, such a trap-assisted tunneling (TAT) current is responsible for a reverse current in irradiated structures — Fig. 1(a) and (c).

In fact, according to [69–71], the bias dependence of the TAT current is described by

$$I_R = I_{0,\text{TAT}}(U_d - V)\exp\left(-\frac{R_{\text{TAT}}}{F_m}\right),\tag{7}$$

where $I_{0,\text{TAT}}$ and R_{TAT} do not depend on voltage, $I_{0,\text{TAT}}$ is proportional to the trap concentration and U_d is the barrier height. The reverse I-V branches for irradiated structures before and after UST were fitted to Eq. (7). It is seen in Fig. 1 that the experimental data are in a good agreement with the fitting curves, which thus confirms the above assumption that the reverse current mechanism is involved. The current deviation at high bias is probably caused by series resistance.

Analysing the deduced parameters listed in Table 1, one can see that UST leads to decrease in the $I_{0,\text{TAT}}$ and barrier height values. The former is evidently due to low temperature acousto-annealing of radiation

traps (E' centers). This can be thought to come from acoustically stimulated diffusion of interstitial oxygen and hydrogen atoms. The barrier lowering is obviously in agreement with P_b annealing mentioned above.

The analysis also show that γ-irradiation results in considerable degradation of the rectification factor K_{RECT}. But UST leads to a forward current increase as well as reverse current decrease in irradiated Au-SiO$_2$-Si structures. Weighing the K_{RECT} data at 0.5 V listed in Table 1, we conclude that the recovery of K_{RECT} is observed due to UST. Thereby, a partial recovery of γ-degraded Si-MOS structure properties by ultrasound treatment is observed at temperatures close to room temperature.

4. Conclusion

The influence of γ-irradiation and ultrasound treatment on current mechanisms in Au-SiO$_2$-Si structures is experimentally studied. In the non-treated structures, the thermionic emission and tunneling through the SiO$_2$ layer contribute to the current. It is shown that γ-irradiation results in appearance of the space charge limited current at forward bias and trap-assisted tunneling current at reverse bias as well as in attenuation of the thermionic emission current. It is revealed that ultrasound treatments at temperatures close to room temperature increase the rectification factor value. The observed acoustically induced variation of the current is indicative of a low-temperature (≈80 °C) annealing of the P_b and E' centers. These observations can be explained by an enhanced diffusivity of interstitial species (hydrogen and oxygen) under ultrasound loading conditions. Taking into account the observed increase in the power-law parameter for a space charge limited current it can be concluded that ultrasound treatment narrows the energy distribution of γ-induced traps at the Si/SiO$_2$ interface. Thus, ultrasound can be an effective tool for controlling metal-semiconductor structure characteristics.

Declaration of Competing Interest

The authors declare that they have no known competing financial interests or personal relationships that could have appeared to influence the work reported in this paper.

Appendix A. Supplementary data

Supplementary data associated with this article can be found, in the online version, at https://doi.org/10.1016/j.sse.2019.107712.

References

[1] Rao A, Krishnan S, Sanjeev G, Siddappa K. Effect of 8 Mev electrons on Au/n–Si Schottky diodes. Int J Pure Appl Phys 2009;5(1):55–62.

[2] İlke Taşçıoğlu A, Tataroğlu A Özbay, Altndal Şemsettin. The role of ^{60}Co γ–ray irradiation on the interface states and series resistance in MIS structures. Radiat Phys Chem 2010;79(4):457–61. https://doi.org/10.1016/j.radphyschem.2009.10.002.

[3] Tataroğlu A, Antindal Ş. Analysis of interface states and series resistance at MIS structure irradiated under ^{60}Co γ–rays. Nucl Instrum Methods Phys Res Sect A 2007;580(3):1588–93. https://doi.org/10.1016/j.nima.2007.07.027.

[4] Olikh OY. Non-monotonic γ– ray influence on Mo/n-Si Schottky barrier structure properties. IEEE Trans Nucl Sci 2013;60(1):394–401. https://doi.org/10.1109/TNS.2012.2234117.

[5] Verma S, Praveen KC, Bobby A, Kanjilal D. Recovery of electrical characteristics of Au/n–Si Schottky junction under ^{60}Co gamma irradiation. IEEE Trans Device Mater Reliab 2014;14(2):721–5. https://doi.org/10.1109/TDMR.2014.2312753.

[6] Salari MA, Güzeldir B, Salam M. The effects of gamma irradiation on electrical characteristics of zn/zno/n-si/au-sb structure. AIP Conf Proc 2018;1935(1):050002 https://doi.org/10.1063/1.5025974.

[7] Podolian AO, Nadtochiy AB, Korotchenkov OA. Charge carrier lifetime recovery in γ– irradiated silicon under the action of ultrasound. Tech Phys Lett 2012;38(5):405–8. https://doi.org/10.1134/S1063785012050124.

[8] Podolyan A, Khivrich V. Room–temperature ultrasonic annealing of radiation defects in silicon. Tech Phys Lett 2005;31(10):11–6. https://doi.org/10.1134/1.1931783.

[9] Olikh Y, Tymochko M, Dolgolenko A. Acoustic–wave–stimulated transformations of radiation defects in γ–irradiated n–type silicon crystals. Tech Phys Lett 2006;32(7):586–9. https://doi.org/10.1134/S106378500607011X.

[10] Olikh Y, Karas' N. On the effect of ultrasound on the annealing of radiation defects in neutron–doped germanium. Fizika i tekhnika poluprovodnikov 1996;30(8):1455–9.

[11] Olikh Y, Tartachnik V, Tichyna I, Vernidub R. Termoacoustic annealing of radia-tion–induced defects in indium–phosphide crystal. The proceeding of 5ᵗʰ conference Acoustoelectronics' 91. 1991. p. 95–6. Varna, Bulgaria.

[12] Ostrovskii I, Korotchenkov O, Lysysh VA. Annealing of point defects by ultrasound in solids. Sov Phys Solid State 1987;20(7):2153–6.

[13] Ostrovskii I, Ostrovskaya N, Korotchenkov O, Reidy J. Radiation defects manip-ulation by ultrasound in ionic crystals. IEEE Trans Nucl Sci 2005;52(6):3068–73. https://doi.org/10.1109/TNS.2005.861476.

[14] Davletova A, Karazhanov SZ. A study of electrical properties of dislocation en-gineered Si processed by ultrasound. J Phys Chem Solids 2009;70(6):989–92. https://doi.org/10.1016/j.jpcs.2009.05.009.

[15] Davletova A, Karazhanov SZ. Open-circuit voltage decay transient in dislocation-engineered Si p–n junction. J Phys D: Appl Phys 2008;41(16):165107 https://doi.org/10.1088/0022-3727/41/16/165107.

[16] Guseynov N, Olikh Y, Askerov S. Ultrasonic treatment restores the photoelectric parameters of silicon solar cells degraded under the action of ⁶⁰Co gamma radia-tion. Tech Phys Lett 2007;33(1):18–21. https://doi.org/10.1134/S1063785007010063.

[17] Olikh OY, Gorb AM, Chupryna RG, Pristay-Fenenkov OV. Acousto–defect interac-tion in irradiated and non–irradiated silicon n^+–p structure. J Appl Phys 2018;123(16):161573 https://doi.org/10.1063/1.5001123.

[18] Konoreva O, Lytovchenko M, Malyi Y, Olikh Y, Petrenko I, Pinkovska M, Tartachnyk V. Acoustic–stimulated relaxation of $GaAs_{1-x}P_x$ LEDs electro-luminescence intensity. Semicond Phys Quantum Electron Optoelectron 2016;19(1):34–8. https://doi.org/10.15407/spqeo19.01.034.

[19] Konoreva O, Olikh YM, Pinkovska M, Radkevych O, Tartachnyk V, Shlapatska V. The influence of acoustic–dislocation interaction on intensity of the bound exciton recombination in initial and irradiated GaAsP LEDs structures. Superlattices Microstruct 2017;102:88–93. https://doi.org/10.1016/j.spmi.2016.12.026.

[20] Pashaev IG. Study of the relaxation of the excess current in silicon schottky diodes. Semiconductors 2014;48(10):1391–4. https://doi.org/10.1134/S1063782614100224.

[21] Olikh O. Reversible influence of ultrasound on γ–irradiated Mo/n-Si Schottky bar-rier structure. Ultrasonics 2015;56:545–50. https://doi.org/10.1016/j.ultras.2014.10.008.

[22] Ostapenko S, Jastrzebski L, Lagowski J, Smeltzer RK. Enhanced hydrogenation in polycrystalline silicon thin films using low–temperature ultrasound treatment. Appl Phys Lett 1996;68(20):2873–5. https://doi.org/10.1063/1.116353.

[23] Kropman D, Seeman V, Dolgov S, Medvids A. Effect of ultrasonic treatment on the defect structure of the Si–SiO₂ system. Phys Status Solidi C 2016;13(10–12):793–7. https://doi.org/10.1002/pssc.201600052.

[24] Zaveryukhina N, Zaveryukhina E, Vlasov S, Zaveryukhin B. Acoustostimulated changes in the density of surface states and their energy spectrum in p–type silicon single crystals. Tech Phys Lett 2008;34(3):241–3. https://doi.org/10.1134/S106378500803019X.

[25] Parchinskii P, Vlasov S, Ligai L, Shchukina OY. The effect of ultrasonic treatment on the generation characteristics of a Si–SiO₂ interface. Tech Phys Lett 2003;29(5):392–4. https://doi.org/10.1134/1.1579804.

[26] Zdebsky A, Kropman D, Sheynkman M. The effect of ultrasound on point defects in structures Si–Sio₂. Zh Tekh Fiz 1989;59(8):131–4.

[27] Gorb A, Korotchenkov O, Olikh O, Podolian A. Ultrasonically recovered perfor-mance of γ–irradiated metal-silicon structures. IEEE Trans Nucl Sci 2010;57(3):1632–9. https://doi.org/10.1109/TNS.2010.2047655.

[28] Parchinskii PB, Vlasov SI, Muminov RA, Ismailov KK, Turgunov U. The effect of ultrasound on the parameters of metal–dielectric–semiconductor structures. Tech Phys Lett 2000;26(10):420–2. https://doi.org/10.1134/1.1262865.

[29] Parchinskii P, Vlasov S, Ligai L. Effect of ultrasonic treatment on the generation characteristics of irradiated silicon–silicon–dioxide interface. Semiconductors 2006;40(7):808–11. https://doi.org/10.1134/S106378260607013X.

[30] Collett KA, Bonilla RS, Hamer P, Bourret-Sicotte G, Lobo R, Kho T, Wilshaw PR. An enhanced anleal process to produce SRV <1 cm/s in 1Ω cm n–type Si. Sol Energy Mater Sol Cells 2017;173:50–8. https://doi.org/10.1016/j.solmat.2017.06.022.

[31] Kerr MJ, Cuevas A. Very low bulk and surface recombination in oxidized silicon wafers. Semicond Sci Technol 2001;17(1):35–8. https://doi.org/10.1088/0268-1242/17/1/306.

[32] Aberle AG. Surface passivation of crystalline silicon solar cells: a review. Prog Photovoltaics Res Appl 2000;8(5):473–87. https://doi.org/10.1002/1099-159X(200009/10)8:5<473::AID-PIP337>3.0.CO;2-D.

[33] Larionova Y, Mertens V, Harder N-P, Brendel R. Surface passivation of n–type Czochralski silicon substrates by thermal–SiO₂/plasma–enhanced chemical vapor deposition SiN stacks. Appl Phys Lett 2010;96(3):032105 https://doi.org/10.1063/1.3291681.

[34] Angermann H, Balamou P, Lu WJ, Korte L, Leendertz C, Stegemann B. Oxidation of Si surfaces: effect of ambient air and water treatments on surface charge and in-terface state density. Ultra Clean Processing of Semiconductor Surfaces XIII, Vol. 255 of Solid State Phenomena 2016. p. 331–7. https://doi.org/10.4028/www.scientific.net/SSP.255.331.

[35] Philipossian A. Activity of HF/H₂O treated silicon surfaces in ambient air before and after gate oxidation. J Electrochem Soc 1992;139(10):2956–61.

[36] Morita M, Ohmi T, Hasegawa E, Kawakami M, Ohwada M. Growth of native oxide on a silicon surface. J Appl Phys 1990;68(3):1272–81. https://doi.org/10.1063/1.347181.

[37] Sze SM, Lee M. Semiconductor devices: physics and technology. 3rd ed. New York: John Wiley & Sons Inc; 2012.

[38] Pershenkov V, Popov V, Shalnov A. Poverkhnostnye radiatsiyni efekty v elementakh intehralnykh mikroskhem. Moskow: Enerhoatomyzdat; 1988.

[39] Karaboga N, Kockanat S, Dogan H. The parameter extraction of the thermally an-nealed schottky barrier diode using the modified artificial bee colony. Appl Intell 2013;38(3):279–88. https://doi.org/10.1007/s10489-012-0372-x.

[40] Rhoderick EH, Williams RH. Metal-semiconductor contacts. 2nd ed. Oxford: Clarendon Press; 1988.

[41] Andrews J, Lepselter M. Reverse current-voltage characteristics of metal-silicide Schottky diodes. Solid-State Electron 1970;13(7):1011–23. https://doi.org/10.1016/0038-1101(70)90098-5.

[42] Ozbek AM, Baliga BJ. Tunneling coefficient for GaN Schottky barrier diodes. Solid-State Electron 2011;62(1):1–4. https://doi.org/10.1016/j.sse.2011.04.016.

[43] Kobayashi H, Ishida T, Nakato Y, Mori H. Mechanism of carrier transport through a silicon–oxide layer for indium–tin–oxide/silicon–oxide/silicon solar cells. J Appl Phys 1995;78(6):3931–9. https://doi.org/10.1063/1.359912.

[44] Novikov YN. Non-volatile memory based on silicon nanoclusters. Semiconductors 2009;43(8):1040–5. https://doi.org/10.1134/S1063782609080144.

[45] Niu G, Banerjee G, Cressler JD, Roldan JM, Clark SD, Ahlgren DC. Electrical probing of surface and bulk traps in proton-irradiated gate–assisted lateral PNP transistors. IEEE Trans Nucl Sci 1998;45(6):2361–5. https://doi.org/10.1109/23.736455.

[46] Pintilie I, Fretwurst E, Lindström G, Stahl J. Second–order generation of point de-fects in gamma–irradiated float-zone silicon, an explanation for type inversion. Appl Phys Lett 2003;82(13):2169–71. https://doi.org/10.1063/1.1564869.

[47] Ma D-H, Zhang W-J, Luo R-Y, Jiang Z-Y, Qiang-Ma X-B, Ma Z-Q, Fan D-Y, Song L Zhang. Effect of si nanoparticles on electronic transport mechanisms in p-doped silicon-rich silicon nitride/c-si heterojunction devices. Mater Sci Semicond Process 2016;50:20–30. https://doi.org/10.1016/j.mssp.2016.04.001.

[48] Jafar MMA-G. High-bias current–voltage–temperature characteristics of undoped rf magnetron sputter deposited boron carbide (B_5C)/p–type crystalline silicon het-erojunctions. Semicond Sci Technol 2003;18(1):7–22. https://doi.org/10.1088/0268-1242/18/1/302.

[49] Kaya M, Çetin H, Boyarbay B, Gök A, Ayyildiz E. Temperature dependence of the current–voltage characteristics of Sn/PANI/p–Si/Al heterojunctions. J Phys: Condens Matter 2007;19(40):406205. https://doi.org/10.1088/0953-8984/19/40/406205.

[50] Cantin JL, von Bardeleben HJ, Autran JL. Irradiation effects in ultrathin Si/SiO₂ structures. IEEE Trans Nucl Sci 1998;45(3):1407–11. https://doi.org/10.1109/23.685215.

[51] Devine RAB. The structure of SiO₂, its defects and radiation hardness. IEEE Trans Nucl Sci 1994;41(3):452–9. https://doi.org/10.1109/23.299784.

[52] Lenahan PM, Conley JF. What can electron paramagnetic resonance tell us about the Si/SiO₂ system? J Vac Sci Technol B 1998;16(4):2134–53. https://doi.org/10.1116/1.590301.

[53] Mahapatra S, Saha D, Varghese D, Kumar PB. On the generation and recovery of interface traps in MOSFETs subjected to NBTI, FN, and HCI stress. IEEE Trans Electron Devices 2006;53(7):1583–92. https://doi.org/10.1109/TED.2006.876041.

[54] Esseni D, Bude JD, Selmi L. On interface and oxide degradation in VLSI MOSFETs. i. deuterium effect in CHE stress regime. IEEE Trans Electron Devices 2002;49:247–53. https://doi.org/10.1109/16.981214.

[55] Fleetwood DM, Pantelides ST, Schrimpf RD, editors. Defects in microelectronic materials and devices. London, New York: CRC Press; 2009.

[56] Schroder DK, Babcock JA. Negative bias temperature instability: road to cross in deep submicron silicon semiconductor manufacturing. J Appl Phys 2003;94(1):1–18. https://doi.org/10.1063/1.1567461.

[57] Parchinskii PB, Vlasov SI, Nasirov A. The effect of γ–ray radiation on the char-acteristics of the interface between silicon and lead–borosilicate glass. Semiconductors 2004;38(11):1304–7. https://doi.org/10.1134/1.1823064.

[58] Jivanescu M, Romanyuk A, Stesmans A. Influence of in suti applied ultrasound during Si^+ implantation in Sio₂ on paramagnetic defect generation. J Appl Phys 2010;107(11):114307 https://doi.org/10.1063/1.3369041.

[59] Korotchenkov O, Grimmeiss H. Long-wavelength acoustic-mode-enhanced electron emission from Se and Te donors in silicon. Phys Rev B 1995;52(20):14598–606. https://doi.org/10.1103/PhysRevB.52.14598.

[60] Olikh OY. The variation in activity of recombination centers in silicon p–n struc-tures under the conditions of acoustic loading. Semiconductors 2009;43(6):745–50. https://doi.org/10.1134/S1063782609060116.

[61] Olikh OY, Voytenko KV, Burbelo RM. Ultrasound influence on I-V–T characteristics of silicon Schottky barrier structure. J Appl Phys 2015;117(4):044505 https://doi.org/10.1063/1.4906844.

[62] Savkina R, Smirnov A, Kryshtab T, Kryvko A. Sonosynthesis of microstructures array for semiconductor photovoltaics. Mater Sci Semicond Process 2015;37:179–84. https://doi.org/10.1016/j.mssp.2015.02.066.

[63] Takakura K, Ohyama H, Ueda A, Nakabayashi M, Hayama K, Kobayashi K, Simoen E, Mercha A, Claeys C. Recovery behaviour resulting from thermal annealing in n–MOSFETs irradiated by 20 MeV protons. Semicond Sci Technol 2003;18(6):506–11. https://doi.org/10.1088/0268-1242/18/6/319.

[64] Wurzer H, Mahnkopf R, Klose H. Annealing of degraded npn–transistors-mechan-isms and modeling. IEEE Trans Electron Devices 1994;41(4):533–8. https://doi.org/10.1109/16.278506.

[65] Koshka J, Ostapenko S, Ruf T, Zhang JM. Activation of luminescence in poly-crystalline silicon thin films by ultrasound treatment. Appl Phys Lett 1996;69(17):2537–9. https://doi.org/10.1063/1.117731.

[66] Ostapenko SS. Mechanism of ultrasonic enhanced hydrogenation in poly–Si thin films. Defects in Semiconductors 19, Vol. 258 of Materials Science Forum Trans Tech Publications; 1997. p. 197–202. https://doi.org/10.4028/www.scientific.net/MSF.258-263.197.

[67] Aziz MJ. Stress effects on defects and dopant diffusion in Si. Mater Sci Semicond Process 2001;4(5):397–403. https://doi.org/10.1016/S1369-8001(01)00014-2.

[68] DiMaria DJ, Cartier E. Mechanism for stress–induced leakage currents in thin silicon dioxide films. J Appl Phys 1995;78(6):3883–94. https://doi.org/10.1063/1.359905.

[69] Gilmore AS, Bangs J, Gerrish A. I-V modeling of current limiting mechanisms in HgCdTe FPA detectors. Proc SPIE 2004;5563:46–54. https://doi.org/10.1117/12.562614.

[70] Gopal V, Singh SK, Mehra RM. Excess dark currents in HgCdTe p^+–n junction diodes. Semicond Sci Technol 2001;16(5):372–6. https://doi.org/10.1088/0268-1242/16/5/316.

[71] Gopal V. A new approach to investigate leakage current mechanisms in infrared photodiodes from illuminated current–voltage characteristics. J Appl Phys 2014;116(8):084502 https://doi.org/10.1063/1.4893899.

Oleg Ya. Olikh was born in Kyiv, Ukraine, in 1974. He received the Ph.D. (2001) and D.Sc. (2018) in solid state physics from Taras Shevchenko National University of Kyiv. Since 2001, he has been an associate professor in the Department of Physics at Taras Shevchenko National University of Kyiv. His research interests in semiconductor physics have focused on external (radiation, ultrasound) influence on properties of semiconductor devices.